Dynamic potential of naval nuclear power generation: modelling of a high-temperature reactor with a supercritical carbon dioxide power conversion cycle

T.H. Wien[ab*], ir. G.-J. Meijn [c]

[a]Delft University of Technology, The Netherlands;
[b]Netherlands Defence Academy, The Netherlands;
[c]Damen Naval - Research Development & Innovation (RDI), The Netherlands
[*]Corresponding author. Email: TH.Wien@mindef.nl

Synopsis

There is a renewed interest in nuclear power generation within the maritime sector as a low-emission power source. As other renewable sources or alternative fuels contain a lower energy density than conventional fossil fuels, and the energy demand of naval vessels will rise due to implementation of unmanned assets and direct energy weapons (DEW), a problem occurs for the limited volume onboard of a naval vessel. Nuclear power generation could play a supplementary role due to its high energy density, while improving the duration of the vessel and thus enhancing operational flexibility and strategic autonomy.

The generation IV very high temperature reactor (VHTR) was selected for implementation due to its enhanced efficiency, safety and relative high TRL compared to other generation IV reactors. In combination with the high efficiency and compact sizing of a supercritical carbon dioxide (sCO_2) Brayton power conversion cycle, could this reactor produce an economically, social and technical feasible option for nuclear power generation.

Nuclear energy is however commonly used as a stable power source, and therefore the question arises if nuclear power generation can provide the dynamic power transients common to a naval vessel. By proposing a novel dynamic model of the nuclear reactor, its power conversion cycle and the vessel itself, this paper investigates the dynamics of a nuclear vessel and determines if implementation of nuclear energy is technologically feasible.

With the proposed model, the transient speed of the nuclear power plant will be compared to conventional prime movers of naval vessels, specifically the diesel engine and gas turbine. Three different control scenarios were analysed; (1) transient reactor control, (2) constant reactor power with dynamic bypass control, and (3) constant reactor power with bypass and additional cooling for reactor temperature management. Results indicate that operating the reactor in transient mode will limit the system dynamics to the dynamics of the reactor, which were deemed not sufficient for power transients in naval vessels. Keeping the reactor at constant power output therefore limits the system dynamics to the bypass in the secondary cycle, but this control method is capable of achieving power transients up and equal to gas turbine level. However, it requires additional cooling of the reactor to prevent a temperature increase within the reactor. Dynamic limitations with this control method do not occur due to the nuclear power plant installation, but by the limitation in the operating envelope of the electric motor. Final results also indicate that fixing the reactor power output to its maximum and thus providing maximum thermal input to the secondary cycle, while operating the secondary cycle itself at part load, significantly lowers the overall plant efficiency. The overall plant efficiency can be improved by modulating the reactor output to match the demand of the secondary cycle, but this again limits the system dynamics to the dynamics of the reactor.

The paper therefore concludes that a VHTR with a sCO_2 Brayton cycle is a promising option for nuclear power generation in naval vessels. With appropriate control strategies and safety measures, nuclear systems can match the dynamic performance of conventional propulsion and power generation systems. Further research should however be committed to improving cycle efficiency at part load and enhancing safety evaluations before nuclear power generation could be deemed a feasible option for naval nuclear power generation.

Keywords: Nuclear power generation; nuclear propulsion; high temperature reactor; supercritical carbon dioxide power conversion cycles; dynamic modelling; power simulations.

Authors' biographies

Sub-Lt (E) Tom Wien is a Naval Officer who graduated in 2022 at the Netherlands Defence Academy for a BSc. in Military Systems and Technology. He is now finishing his MSc. in mechanical engineering at Delft University of Technology, focusing on Energy, Flow and Process Technologies. In his MSc. thesis, he focuses on the dynamic power behaviour of a nuclear power plant installation for implementation on naval vessels. After his thesis, he will finish his Officer's training at the Royal Netherlands Naval College institute and will serve as Technical Officer on the vessels of the Royal Netherlands Navy.

ir. Gert-Jan Meijn is currently the innovation lead for marine and electrical systems at the Research Development and Innovation department of Damen Naval. He received his BSc. and MSc. in mechanical engineering at Delft University of Technology in 2013 and 2015 respectively. In his current role, he is responsible for identifying new technology, initiating innovation projects, and ensuring that new technology is embedded in products and future projects. Experiences in previous roles include the concept design of propulsion plants, vessel performance evaluation, simulation of system dynamics, and the development of novel control algorithms. His research interests include the development of future power and propulsion systems, holistic system simulation, control systems, energy management and sustainable power generation.

1 Introduction

Nuclear power generation has recently gained increasing interest within the maritime sector in the Netherlands and Europe. According to the Dutch maritime sector policy report "No Guts, No Hollands Glorie!" 2023, nuclear energy can help reduce dependency on fossil fuels and provides a potential high-energy density source for ships without emitting carbon dioxide (CO_2). One of the project goals is to develop a standardized, modular nuclear reactor for ship integration within 10 years Dutch maritime sector (2023). The resurgence of interest in nuclear power generation for maritime applications comes at a crucial time when the global shipping industry is aiming to reduce its environmental impact.

Due to the implementation of unmanned assets and direct energy weapons, it is expected that energy usage on naval vessels will not decrease in the coming years Royal Dutch Navy (2023). However, renewable energy sources, like wind and solar, and alternative fuels, like methanol, have a lower energy density compared to conventional fossil fuels van Zalk and Behrens (2018) U.S. Department of Energy (2024). An increasing energy demand while energy density is decreasing results in an energy mismatch problem, presenting an issue for the volume limited environment of a vessel. Nuclear energy could play a major role in solving this issue, as it offers one of the highest available energy densities.

In addition, operational advantages of nuclear power generation arise for naval vessels, as sufficient power for long operation times can be guaranteed. As a result, nuclear vessels can ensure high vessel speeds without losing operational endurance. Operational flexibility is improved compared to conventional vessels, as nuclear ships can respond to crises quicker and can operate longer with fewer logistic support, improving the strategic autonomy of the operator U.S. Department of the Navy and Department of Energy (2015).

Nuclear power generation has been implemented in military ships, such as aircraft carriers, submarines and cruisers by several countries, and has already been applied on merchant vessels like icebreakers and cargo ships, although successes differ significantly Freire and de Andrade (2015). Despite previous usage of nuclear power generation, implementation of the technology in future vessels will present challenges, especially for countries not possessing this classified technology. As nuclear reactors typically operate as stable constant power sources, which contrasts with the fluctuating power demands of (naval) vessels, issues could arise in providing the dynamic power profile of the vessel. To determine the possibility of nuclear power generation as a replacement of conventional fossil fuels, the power dynamics of a nuclear power plant installation must be assessed.

This paper investigates a) the dynamic possibilities of a nuclear power plant installation on a naval vessel, and compares it to dynamics of conventional prime movers of a naval vessel, and, b) indicates potential safety issues during power dynamics of such a power plant and provides preliminary solutions to ensure safe operation. The paper proposes a novel power plant model for dynamic power simulations of a nuclear reactor, its power conversion cycle and the vessel's propulsion system.

In the investigated scenarios, the modelling results demonstrate the power transients that can be achieved with different control methods and which considerations should be made to realize optimal power transients for the nuclear power plant installation. With the proposed modelling strategy, the dynamic possibilities of a nuclear power plant are determined, and additional insights at system level are obtained for further cycle designs.

Lastly, the power transients are projected on a notional frigate design, based on the work of Geertsma (2019), analysing the impact on ship performance. Noting that the requirements for power transients on board of naval vessels are increasingly demanding due to new (direct energy) weapon and sensor technology, this paper also aims to demonstrate the competitiveness of nuclear technology with respect to the conventional prime movers.

2 System description

Nuclear power plants function by using the heat released during nuclear fission inside a nuclear reactor. This heat is converted into mechanical power by means of a thermodynamic power cycle such as a Rankine or a Brayton cycle. Depending on the application, this mechanical power is used directly (e.g. direct mechanical propulsion) or converting the mechanical power first into electrical power using a generator. There are different types of reactors and possible cycle configurations for nuclear power generation, but the most common type of reactor is the pressurised water reactor (PWR). PWR technology is used in over 70% of all operable land based reactors, as it is used in 307 out of the 437 worldwide reactors in 2022 World nuclear association (2023). The typical cycle efficiency of such a power plant (from thermal power to electrical power) is around 33% IAEA (2023), but this depends strongly on the specific type of reactor.
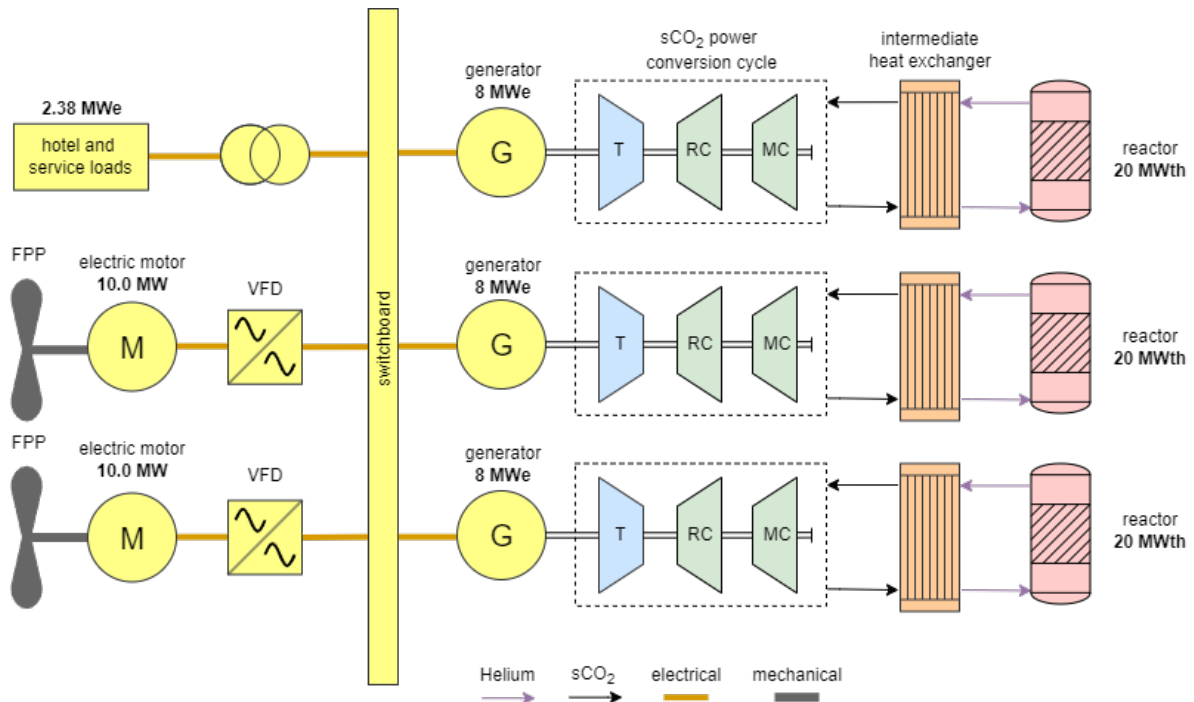
Figure 1: Schematic overview of the electric propulsion plant fed by multiple nuclear power generators

2.1 Ship overview

To determine the dynamic potential of a nuclear power generation system, integration within a naval vessel should occur. For this research, the vessel proposed by Geertsma (2019) was implemented as a preliminary design choice, representing a notional frigate. The design values of this vessel are presented in Table 1. A full-electric propulsion system is proposed, with two large propulsion electric motors driving fixed pitched propellers. The nuclear power generation is split in three individual generator modules (3 x 8 MWe), which together provide power to both the propulsion (2 x 10 MW) and to the vessel's hotel and service loads. The resulting electric propulsion plant is presented in Figure 1, of which the nuclear reactor and its power conversion cycle will be further explained in the sections 2.2 and 2.3. With the current sizing, the installed power is sufficient to fully utilize the propulsion motors and approx. 2+ MWe of hotel and service loads. The notional frigate can reach a speed of 26+ knots.

Table 1: Design values of the notional frigate

Parameter	Value
Ship length [m]	135.0
Displacement [tonnes]	5400
Type of propulsion	Full electric
Max. speed [knots]	26+
Propeller type	2 x FPP (Wageningen C5-75)
Propeller diameter [m]	4.90 m
Propeller pitch (P/D) [-]	1.450
Nuclear power generators [MWe]	3 x 8
Propulsion motors [MW]	2 x 10
Propulsion motor speed [RPM]	120 (nom.) / 135 (max.)

2.2 Propulsion choice

As reactor, the generation IV very high temperature reactor (VHTR) Zohuri (2020) was selected for implementation. The VHTR is a graphite-moderated reactor operating on the thermal neutron spectrum. Its design focus in on maximizing safety and thermal efficiency, the latter by having a high outlet temperature between 700°C and 850°C Zohuri (2020). The reactor applies the TRISO layered particles with UO_2 kernels Olander (2009) IAEA (2023), which has been specifically made for the high temperature environment of the VHTR. The selection of a VHTR is contradicting with the fact that historically almost all the nuclear propelled reactors on board of vessels

apply pressurized water reactors (PWR) as energy source. However, the potential of the VHTR regarding a more efficient Olander (2009)Zohuri (2020), passive safe Zohuri (2020), economically feasible Steigerwald et al. (2023) and relative high technology readiness level (TRL) compared to other gen. IV reactors Gen IV International forum (2014), provides the question if PWRs will be used solely on nuclear vessels in the future.

Naval vessels are permitted to use highly enriched uranium (HEU) in contrary to merchant vessels which can only use low enriched uranium (LEU) fuel, containing an enrichment up to 20% of U-235 World nuclear association (2023). Still, it was decided to implement a LEU fuelled reactor for naval applications as nuclear proliferation risks are reduced and the potential for naval and merchant collaboration towards nuclear vessels remains possible.

Supercritical carbon dioxide (sCO_2) is an attractive fluid for a nuclear power conversion cycle implemented on a naval vessel due to its attractive properties in supercritical state. Above the critical point (73.9 bar and 31.1°C), CO_2 has a liquid-like density, while still having a gas-like viscosity, which ensures power production is more efficient and compact Marchionni et al. (2019). The volume on a (naval) vessel is limited compared to land based applications. The amount of volume needed for sCO_2 turbomachinery is less than other types of turbomachinery. Ming et al. (2023) state that at the same power level, the sCO_2 Brayton cycle is only one-tenth in size compared to the steam Rankine cycle. Further on, at higher turbine inlet temperatures, corresponding to the temperature range of a VHTR, the cycle efficiency of sCO_2 is higher than any other working fluid Wu et al. (2020). Experience with nuclear vessels shows that economics are crucial for successful nuclear ship design Freire and de Andrade (2015), which are improved with a higher cycle efficiency. A higher cycle efficiency also results in needing less fuel for the same amount of energy production, ensuring that the amount of nuclear waste decreases, improving public trust in this technology. Finally, the lower shaft and turbomachinery inertia of the sCO_2 cycle, compared to turbomachinery of other fluids Michael A. Pope (2006) Carstens (2007), could turn beneficial for dynamic power behaviour.

2.3 Cycle design

Implementation of a VHTR within the simulation requires a sufficient developed reactor design. The 10 MWth U-battery was therefore selected, as Atkinson et al. provide the required design parameters within their research Atkinson (2018) Atkinson et al. (2019a) Atkinson et al. (2019b) Atkinson et al. (2021) Atkinson and Aoki (2024). A single 10 MWth reactor will not provide the required power output for typical naval applications, so for that reason it was decided to combine two single 10 MWth U-battery as power source for one power conversion cycle, resulting in a 20 MWth power source for a single power conversion cycle. An overview of the generic U-battery is presented in Table 2. Additionally, a cross-section of the reactor is presented in Figure 2, showing the various layers of the reactors, the flow path through the reactor, and a general indication of the outer dimensions.

Table 2: Design values of the U-battery Atkinson (2018)

Parameter	Value
Reactor type	VHTR
Neutron spectrum	Thermal
Core layout	Prismatic
Moderator	Graphite
Coolant	Helium
Fuel type	UO_2 (TRISO)
Capacity [MWth]	10
Inlet temperature [°C]	400
Outlet temperature [°C]	750
Pressure [bar]	40

Although developments are still ongoing towards the optimal sCO_2 power conversion cycle, the indirect recompression cycle is deemed the most efficient cycle configuration while being relative simplistic Dostal (2004) Carstens (2007) Brun et al. (2017), and was therefore selected as the first tested cycle design configuration. The indirect nuclear sCO_2 recompression cycle designed for naval power generation is presented in Figure 3.
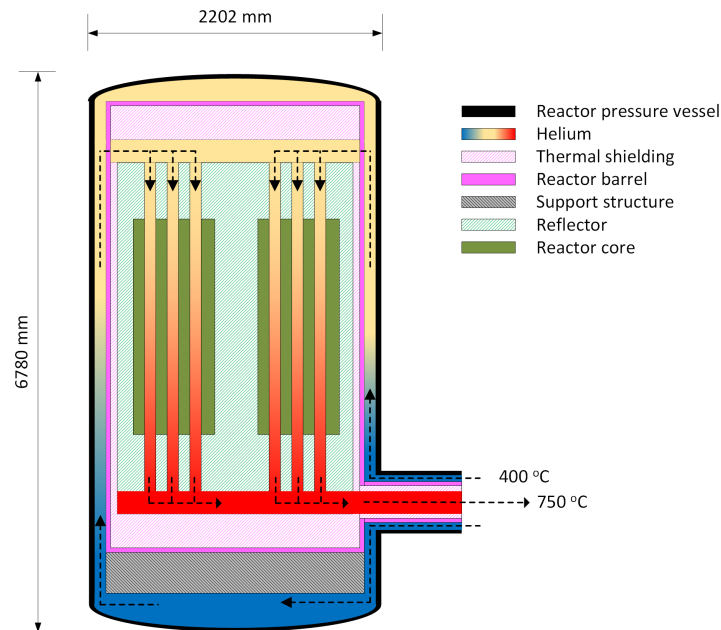
Figure 2: Schematic cross-section of the U-battery based on Ding et al. (2011), design values and sizing taken from Atkinson et al. (2019b) - **note:** figure not drawn to scale
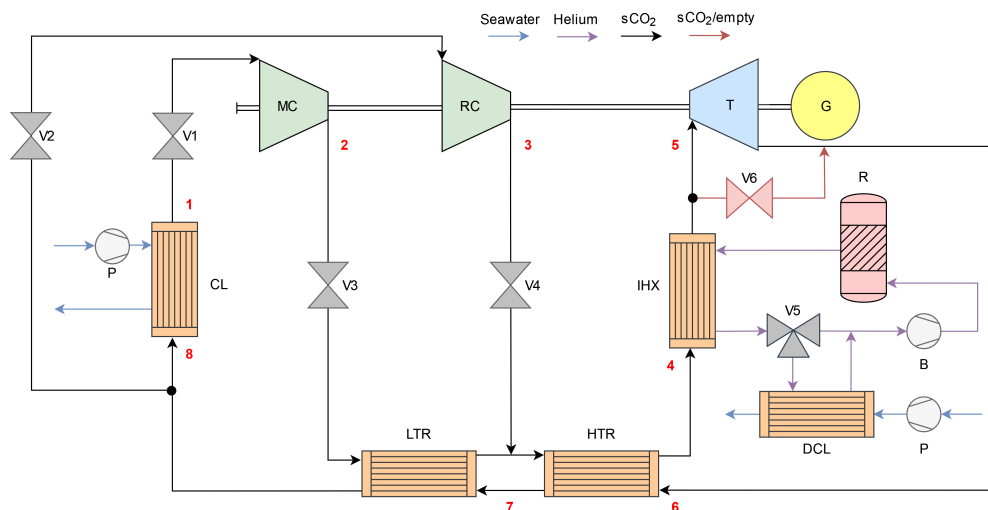

Figure 3: Schematic overview of the designed recompression cycle with a nuclear reactor

The recompression cycle applies a nuclear reactor (R) as heat source, using helium as working medium. This heat will be transferred by the intermediate heat exchanger (IHX) to the sCO$_2$ cycle. The sCO$_2$ cycle applies a single stage turbine (T), but adds another separate compression stage, resulting in a main compressor (MC) and a re-compressor (RC). This turbomachinery is all connected to a single shaft, applying a Turbine-Alternator-Compressor (TAC) configuration, which also drives the generator (G). For optimal cycle efficiency, two recuperators will be implemented after each compressor, resulting in a low and high temperature recuperator (LTR and HTR). A cooler (CL), and an optional dump cooler (DCL), must be implemented to transfer waste heat from the cycle to the seawater. While cooling using an intermediate fresh water circuit would also be a valid option, especially given the high pressures and integrity requirements of the sCO$_2$ cycle, the choice for a seawater cooling loop has been made for the sake of simplicity and reducing the overall number of (intermediate) heat exchangers. The primary loop (reactor loop) and the cooling loops also need an additional pump (P) or blower (B) to ensure sufficient mass flow and pressure within the system. Further on, for dynamic power control multiple valves are present within the system. Throttle valves are placed before and after the compressors (V1-V4) to maintain pressure within desired limits, a three-way valve (V5) is implemented to control mass flow going through the DCL and a bypass valve (V6) is placed around the turbine for load control.

All the heat exchangers within the power conversion cycle are wavy channelled printed circuit heat exchangers (PCHE). This is a widely chosen heat exchanger type for (nuclear) sCO$_2$ power conversion cycles due to its high efficiency Olumayegun et al. (2017)Jiang et al. (2018), capability to withstand high pressures and temperatures Carstens (2007)Wang et al. (2021) and being relatively small compared to other heat exchangers (compared to a shell and tube heat exchanger it needs only 20% of the volume for the same heat load capabilities Ming et al. (2022)). PCHEs also have faster thermal dynamic responses, due to their lower mass and higher heat transfer coefficients compared to shell-and-tube heat exchangers Deng et al. (2019), which makes them beneficial for naval implementation.

Before testing the dynamic behaviour of the recompression cycle, specific design conditions must be selected. The results of this cycle design are presented in Table 3 and Figure 4 Wien (2024). This cycle design is based on the following approach. Firstly, the lower cycle pressure is fixed at 90 bar, as this ensures a sufficient margin is realised from the critical point of CO$_2$. The characteristics of the selected turbomachinery result in a pressure ratio of 2.5, resulting in a high cycle pressure of 225 bar, which is within pressure limits of a sCO$_2$ power conversion cycle Olumayegun and Wang (2019). To ensure that the notional frigate design can operate globally, a seawater inlet temperature of 35°C was selected as the worst case scenario Seatemperature.org (2024). Furthermore, a terminal temperature difference (TTD) for the heat exchanger must be selected, which was assumed to be equal to 10°C for all heat exchangers Olumayegun and Wang (2019). Although a smaller TTD could be beneficial for cycle design, this would increase heat exchanger sizing. Only a full cycle design for implementation on a vessel could determine if additional heat exchanger sizing is permissible, and therefore identification of the optimal TTD balance is not considered in this work.

Table 3: Design values of the power conversion cycle Wien (2024)

Parameter	Value
Working fluid	Supercritical carbon dioxide (sCO$_2$)
Cycle type	Indirect recompression
Turbomachinery type	Radial/centrifugal
Thermal power [MWth]	20.0
Electrical power [MWe]	8.0
Efficiency [%]	40.0
Shaft speed [RPM]	20,000
Cycle pressure [bar]	90–225
Cycle mass flow [kg/s]	114.78
Split ratio [-]	0.71
Seawater inlet temperature [°C]	35
Heat exchanger terminal temperature difference [°C]	10

The eight design points, as presented in Figure 4, are determined based on the following reasoning. Thermophysical property databases only require two of the thermodynamic states to be known to determine any other thermophysical property. As pressure is known for each design point, it is only required to determine one other thermophysical property. The sea inlet temperature, and the TTD, provide the temperature in point 1, which is set to 45°C, ensuring fluid conditions above the critical point of CO$_2$. Design point 2 can then be determined based on the enthalpy difference that results from the performance characteristic of the compressor. The temperatures between point 2 and 8 require a minimal difference equal to the TTD. Repeating this process once again results in the design points 3 and 7. As the U-battery has an inlet temperature equal to 400°C, design point 4 should have a temperature equal to 390°C to account for the TTD. To determine the design points 5 and 6, an iterative process regarding optimal cycle efficiency and energy balance must be applied. For optimal cycle efficiency, the mass flow should be as high as possible, as this increases the power output of the turbomachinery. However, three energy balances related to three heat exchangers should be considered as constraints for identifying the optimal cycle efficiency. Firstly, the IHX must balance the 20 MW heat input from the reactors with the energy difference between point 4 and 5. Secondly, the energy balance over the HTR, design points 6 and 7 in comparison with design points 3 and 4, should be equal. Lastly, the energy balance over the LTR, design points 7 and 8 in comparison with design points 2 and 3, should be equal. Using these constraints, while focusing on optimal cycle efficiency and implementing the turbine characteristic, results in design points 5 and 6, followed by the cycle mass flow and design split ratio.
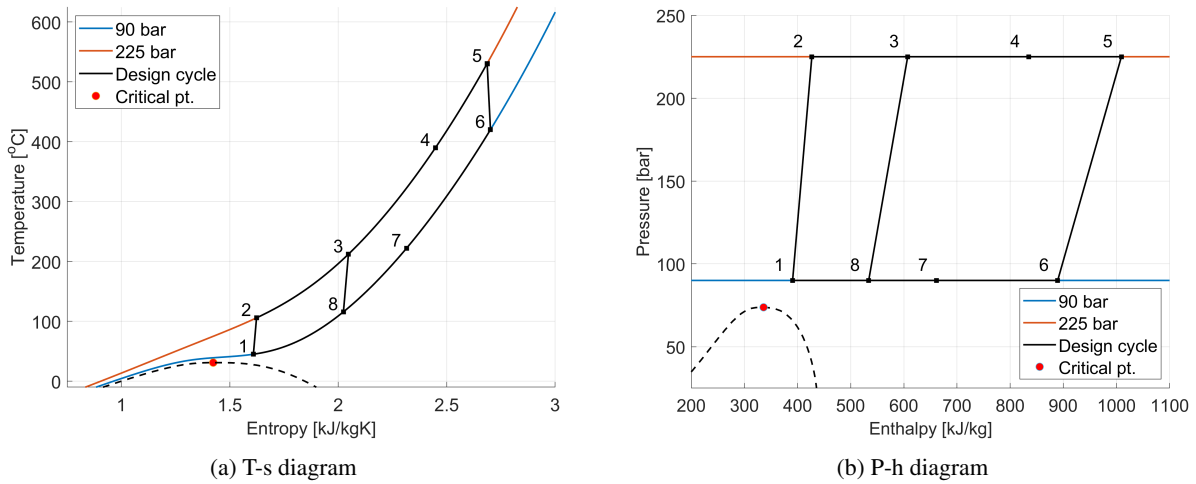
(a) T-s diagram

(b) P-h diagram

Figure 4: Cycle design points for the power conversion cycle

3 Simulation model

Within this section, the dynamic model of the components for the sCO2 closed Brayton cycle for nuclear naval power generation is presented. In order to study the transient performance of the sCO2 plant, and its dynamic possibilities, a dynamic model of the whole system needs to be developed. This includes the nuclear reactor, heat exchangers, turbomachinery, control valves, shaft dynamics and the vessel's propulsion system. It is assumed that the impact of piping is negligible on the dynamic possibilities of the power conversion cycle.

In this work, the individual models are created and connected within the Matlab$^{©}$ and Simulink$^{©}$ working environment, of which an overview is presented in Figure 5. Since Matlab$^{©}$ does not have any thermodynamic and transport property functions, CoolProp$^{©}$ was implemented to calculate the thermophysical properties of the fluids. CoolProp$^{©}$ can be used if two thermodynamic properties are known, so for example the temperature T can be determined if the thermodynamic properties pressure p and enthalpy h are known, which is stated in equation 1.
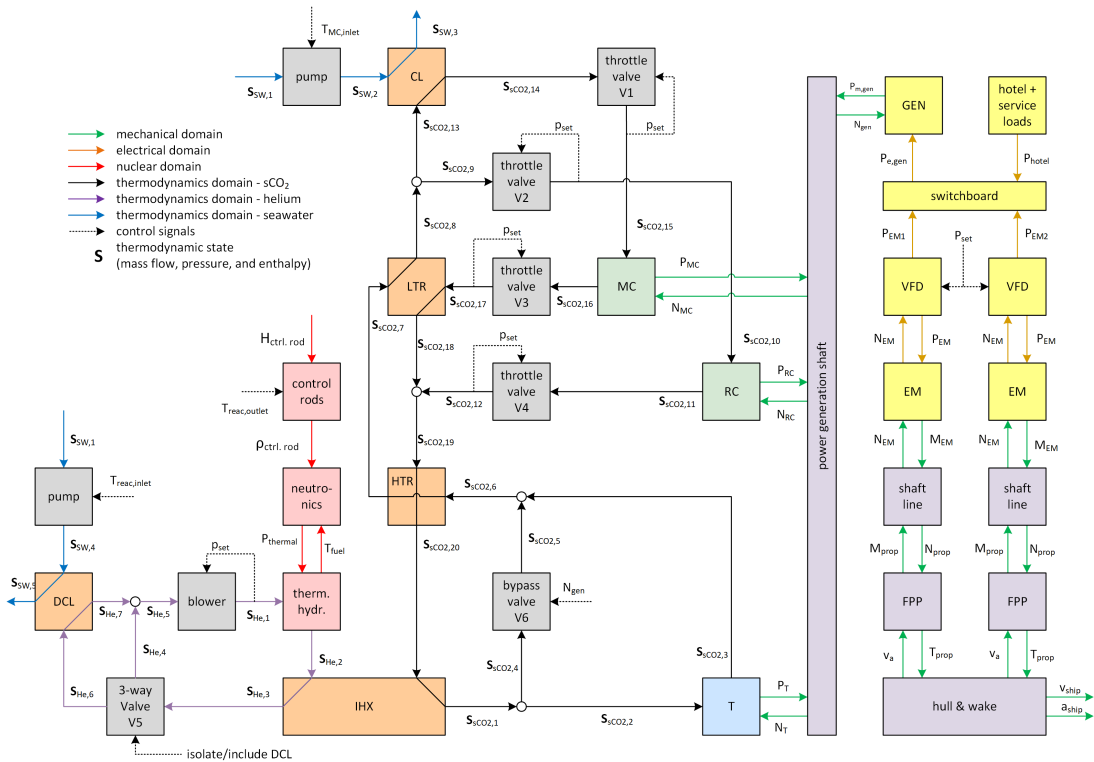
$$T = f(p, h) \tag{1}$$

Figure 5: Model overview of the created nuclear naval power generation system

3.1 Reactor model

For dynamic power simulations of a nuclear reactor, it is important to simulate the neutronics and the thermal hydraulics of a reactor. Neutronics accounts for the fission process occurring within the fuel, while the thermal hydraulic process explains the process of heat being transferred from the fuel to the helium coolant. To control the fission reactions within the reactor, the control rods can be raised or lowered based on the required power output of the reactor.

3.1.1 Neutronics

The process of fission occurring within the reactor is explained by the neutronics of a reactor. A common preliminary modelling method is applying the so called point-kinetics equations (PKEs). The PKEs assume that the spatial dependence of the reactor can be described by a single shape, removing the spatial dependence of the more general neutron diffusion equation Duderstadt and Hamilton (1976). As a result, the neutron density at each point of the nuclear reactor core therefore only varies with time, ensuring dynamic power changes can be simulated by raising or lowering the control rods of the reactor. The PKEs are presented in equation 2 and 3 in their six-group form Duderstadt and Hamilton (1976) Atkinson et al. (2021), and were validated according to Henryk Anglart (2011).

$$\frac{dn}{dt} = \frac{\rho - \beta}{\Lambda} n + \sum_{j=1}^{6} \lambda_j c_j \tag{2}$$

$$\frac{dc_j}{dt} = \frac{\beta_j}{\Lambda} n - \lambda_j c_j, \text{ with } j = 1, 2, \dots 6 \tag{3}$$

Here n is the neutron population, which is related to the thermal power of the reactor, ρ is the change in reactivity, β is the total effective delayed neutron fraction, Λ is the prompt neutron generation lifetime, λ is the effective decay constant and c_j is the concentration of a delayed neutron group Atkinson et al. (2021). Based on a reactor analysis within Serpent, Atkinson et al. (2021) provide the required point kinetic parameters for the U-battery. Furthermore, in addition to the PKEs, the model applies a thermal reactivity feedback system based on a temperature change of the fuel rods. This passive safety feature ensures that reactivity will drop as fuel temperature increases, ensuring power output will lower and fuel temperature will stabilize.
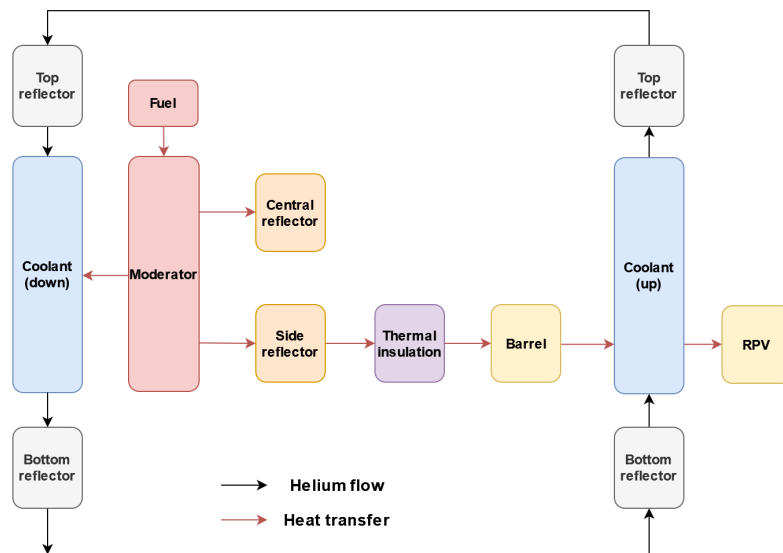
3.1.2 Thermal Hydraulics

Figure 6: Schematic diagram of the lumped thermal hydraulics of the U-battery

The heat generated within the fuel must be transferred to the reactor coolant, which occurs through heat transfer between the different reactor components. To simulate this behaviour, a 1D lumped thermal hydraulics scheme was implemented and validated based on the component structure of the U-battery Atkinson et al. (2019b) Atkinson et al. (2021). The structure of the thermal hydraulics model is presented in Figure 6, which is based on the structure of the reactor as shown in Figure 2. Each component (reactor segment) is modelled by applying mass and energy conservation equations, of which an example for the fuel elements is presented in equation 4.

$$M_F C_F \frac{dT_F}{dt} = Q_{reac} - UA(T_F - T_M) \tag{4}$$

Here, M_F is the mass of the fuel elements, C_F is the specific heat capacity, T_F the fuel temperature, Q_{reac} the heat produced within the fuel elements (determined by the PKEs), U the overall heat transfer coefficient, A the heat transfer area and T_M the temperature of the moderator, which surrounds the fuel elements. Within the reactor, conduction is the main method of heat transfer between the reactor components. Only by interaction with the flowing coolant will convection be part of the overall heat transfer coefficient.

To calculate the overall heat transfer coefficients between the different reactor components, equation 5 is applied Ming et al. (2022). Here, the impact of convection depends on the region in which the fluid operates, which is accounted for by a changing heat transfer coefficient h according to equation 6 Ming et al. (2022). This equation depends on the thermal conductivity k and the thickness t_e of the material, the hydraulic diameter of the channel d_H and the Nusselt Nu number, which is determined by the Gnielinski correlation.

$$\frac{1}{U} = \frac{1}{h_h} + \frac{t_e}{k_w} + \frac{1}{h_c} \tag{5}$$

$$h = \frac{Nu\, k}{d_H} \tag{6}$$

Furthermore, the helium within the reactor flows through channels made within the reflector and hexagonal fuel blocks. As a result, a pressure drop will be realised, which can be calculated according to equation 7. Here, the pressure drop Δp is related to the pressure drop due to a height difference Δh and a friction component. For the friction component holds that the pressure drop depends on the friction factor f, which is calculated by the Petukhov relation, the density of the fluid ρ, the flow speed u, the length of the channel L and the hydraulic diameter d_H of the channel.

$$\Delta p = \Delta p_{height} + \Delta p_{friction} = \rho g \Delta H + \frac{f \rho u^2 L}{2 d_H} \tag{7}$$

3.2 Heat exchanger model

To ensure the thermal inertia of the heat exchangers are accurately implemented within the system, it is of importance to construct a dynamic heat exchanger model. It is common to split the model of the heat exchanger into several nodes and apply a 1D finite volume method on only two channels (one hot and one cold) of the heat exchanger. These channels will be separated by the wall of the heat exchanger and will also be divided into several nodes (n) along the length of the channel, to ensure accurate calculations of the thermal properties. The heat exchangers are modelled as a 20 node structure as this results in the best optimum regarding accuracy and simulation speed Wien (2024), and were validated based on the PCHE of Marchionni et al. (2019).

$$M_h \frac{dh_h}{dt} = \dot{m}_{h,i} h_{h,i} - \dot{m}_{h,o} h_{h,o} - Q_{hw,n} \tag{8}$$

$$M_c \frac{dh_c}{dt} = \dot{m}_{c,i} h_{c,i} - \dot{m}_{c,o} h_{c,o} + Q_{wc,n} \tag{9}$$

For the energy balance within the channels, the energy conservation equations 8 and 9 are applied to each node for the hot (h) and cold (c) channel. In these equations h_i and h_o are the enthalpy of the inlet and outlet fluid of each node. Furthermore, M_h and M_c are the mass of the fluid in the hot and cold side of the heat exchanger. The heat transfer between these two channels occurs between the hot channel and the wall $Q_{hw,n}$ and between the wall and the cold channel $Q_{wc,n}$ according to equations 10 and 11. Ming et al. (2022)

$$Q_{hw,n} = U_{h,n} A_{h,n} (T_{h,n} - T_{w,n}) \tag{10}$$

$$Q_{wc,n} = U_{c,n} A_{c,n} (T_{w,n} - T_{c,n}) \tag{11}$$

In equation 10 and 11 the temperature of the fluid in the heat transfer elements ($T_{h,n}$ or $T_{c,n}$) is equal to the average temperature between the inlet and outlet temperature of the node. To calculate the wall temperature $T_{w,n}$ of the heat exchanger, the energy conservation equation is applied to the wall, which is presented in equation 12 Ming et al. (2022).

$$M_{w,n} C_{w,n} \frac{dT_{w,n}}{dt} = Q_{hw,n} - Q_{wc,n} \tag{12}$$

The overall heat transfer coefficient is calculated based on equations 5 and 6, but this time applying the Gnielinski correlation corrected for a wavy channel for the Nusselt number, as described by Marchionni et al. (2019). The pressure drop along the channels of the heat exchanger can be calculated according to equation 7 Ming et al. (2022) Furlong et al. (2024). Here, the friction factor is calculated according to the Serghides's solution, which is an approximation of the Colebrook–White equation Marchionni et al. (2019).

3.3 Turbomachinery model

(a) Pressure ratio map of the compressor

(b) Efficiency map of the compressor

(c) Pressure ratio map of the turbine
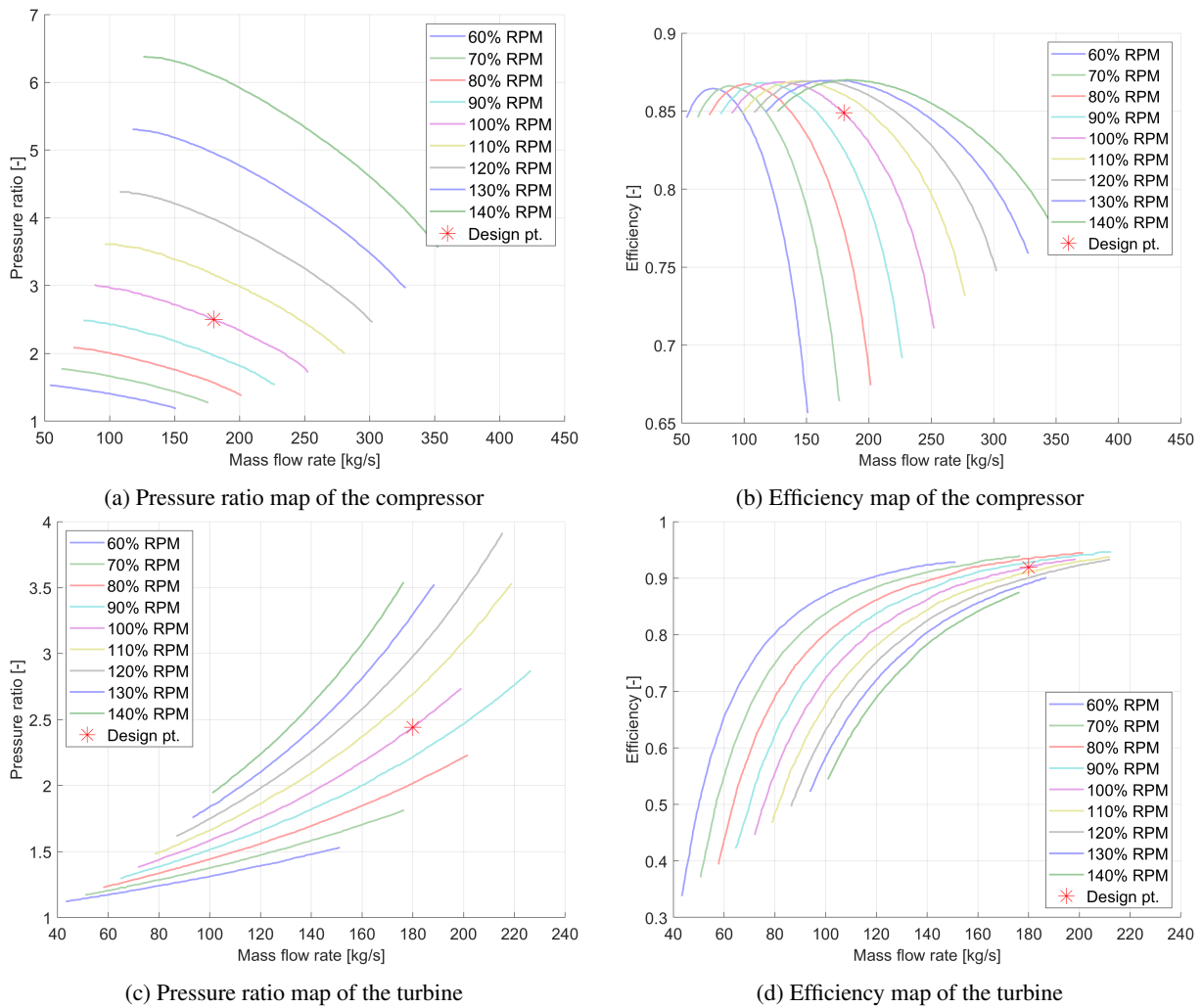
(d) Efficiency map of the turbine

Figure 7: Performance maps of the sCO$_2$ turbomachinery Oh et al. (2016)

Due to the fast response time of the turbomachinery, compared with the heat exchangers and reactor, it is common to neglect the response time of turbomachinery in dynamic simulations Brun et al. (2017)Wang et al. (2021). Therefore, the compressors and turbine are modelled by employing performance characteristic maps for the prediction of the efficiency and pressure ratio, of which the implementation was validated according to Oh et al. (2016). Based on the performance maps of sCO$_2$ turbomachinery created by Oh et al. (2016), presented in Figures 7(a-d), a normalization approach results in the needed performance maps for the designed power conversion cycle. However, as the performance maps are created by specific inlet conditions (pressure and temperature) and dynamic simulations could result in different operating conditions, and thus different turbomachinery performance, a correction equation must be applied to justify the use of the performance maps. Due to the real gas properties of CO$_2$, and the significant changes in thermophysical properties especially near the critical point, the correction equations created by Pham et al. (2016) were implemented. As a result, the performance maps can be used according to equations 13 and 14.

$$\pi = f_{map}(\dot{m}_{corr}, N_{corr}) \tag{13}$$

$$\eta = f_{map}(\dot{m}_{corr}, N_{corr}) \tag{14}$$

Here, the corrected mass flow $\dot{m}_{corr}$ and the corrected shaft speed N_{corr} are used to obtain the pressure ratio π and efficiency η of the turbomachinery. The pressure ratio ensures pressure at the outlet of the compressors and turbine can be determined. Furthermore, enthalpy h at the outlet of the turbomachinery can be calculated according to equations 15 and 16 Alsawy et al. (2024). Here, the isentropic enthalpy h_{isen} can be determined according to equation 17, which uses the fact that for a reversible process entropy s is constant.

$$h_{C,o} = h_{C,i} + \frac{h_{C,o,isen} - h_{C,i}}{\eta_C} \tag{15}$$

$$h_{T,o} = h_{T,i} - \eta_T (h_{T,i} - h_{T,o,isen}) \tag{16}$$

$$s = f(h_i, p_i) \rightarrow h_{o,isen} = f(s, p_o) \tag{17}$$

Finally, the total power produced/consumed by the turbomachinery can be determined according to an energy balance over the system, which results in equations 18 and 19 for the compressor and turbine respectively. Here, the power P of the system is calculated according to the mass flow $\dot{m}$ going through the system and the enthalpy difference between the inlet and outlet.

$$P_C = \dot{m}_C (h_{C,o} - h_{C,i}) \tag{18}$$

$$P_T = \dot{m}_T (h_{T,i} - h_{T,o}) \tag{19}$$

3.4 Shaft and generator model

For a recompression cycle applying a TAC configuration, the rotating speeds of the turbine, compressor and external load are the same. As a result, the shaft speed will only change by a change in positive torque generated by the turbine or a negative torque generated by the compressors or external load Ming et al. (2022). Therefore, the transient behaviour of the shaft can be determined according to equation 20 Oh et al. (2016) Olumayegun and Wang (2019) Ming et al. (2023).

$$I\omega \frac{d\omega}{dt} = P_T - P_{MC} - P_{RC} - P_G \tag{20}$$

The shaft speed dynamics of the power conversion cycle can be calculated according to the inertia I, the shaft speed ω and the power P of the different components connected to the shaft. Although load demand is an electrical power demand, the generator power P_G refers to the mechanical power required by the generator. It is further assumed that the dynamics of the generator can be neglected. Michael A. Pope (2006) determined the shaft inertia belonging to a 2400 MWth nuclear power plant connected to a sCO$_2$ power conversion cycle. To determine the inertia values for the selected power conversion cycle, the inertia values of Pope can be scaled based on the thermal power of the nuclear reactors Oh et al. (2016).

3.5 Control valves

The pressure difference over a throttle and bypass valve is significantly different. Throttle valves are located between pipes that contain similar pressure levels, resulting in low pressure differences, while bypass valves are connected between the high and low pressure side of the power conversion cycle, resulting in large pressure differences. For a throttle valve, it is common that the pressure drop is equal to 0.3-0.6 of the total pressure drop over the piping in which it is located Bian et al. (2022). For a small pressure difference, the case of a throttle valve, equation 21 can be used. For a bypass valve, the mathematical model of an orifice plate flow with a large pressure difference can be used, which is presented in equation 22. In these equations the mass flow is related to a constant valve construction coefficient C_v, the relative opening area of the valve f_{open}, the flow density ρ, the pressure difference between the inlet p_i and outlet p_o of the valve and the specific heat ratio γ Bian et al. (2022).

$$\dot{m} = C_v f_{open} \sqrt{2\rho (p_i - p_o)} \tag{21}$$

$$\dot{m} = C_v f_{open} \sqrt{\frac{2\gamma}{\gamma-1} \rho_i p_i ((\frac{p_o}{p_i})^{\frac{2}{\gamma}} - (\frac{p_o}{p_i})^{\frac{\gamma+1}{\gamma}})} \text{ , for } (\frac{2}{\gamma+1})^{\frac{\gamma}{\gamma-1}} \leq \frac{p_o}{p_i} < 1 \tag{22}$$

$$\dot{m} = C_v f_{open} (\frac{2}{\gamma+1})^{\frac{\gamma+1}{2(\gamma-1)}} \sqrt{\gamma\rho_i p_i} \text{ , for } \frac{p_o}{p_i} < (\frac{2}{\gamma+1})^{\frac{\gamma}{\gamma-1}}$$

3.6 Propulsion plant

In order to investigate what the power dynamics of the indirect sCO$_2$ Brayton cycle would provide in terms of ship performance, a simplified presentation of the full-electric ship propulsion plant and 1 Degree Of Freedom (1-DOF) ship model is included. The electric power generated by the three nuclear generator units is distributed, transformed and partially converted into mechanical power for propulsion. Variable Frequency Drives (VFDs) regulate the mechanical power output of the propulsion motors.

3.6.1 Electric grid and motors

It is assumed that the dynamics of the AC-grid can be neglected, reducing the model to a power balance with fixed efficiencies assumed for each of the components, as presented by equation 23. The electrical power provided by the generators $P_{Gj}\eta_G$ is equal to the power P_{hotel} consumed by hotel and ship service, considering transformer efficiency η_{trans}, added to the power consumed by the electric motors P_{EMj}, considering VFD efficiency η_{VFD} and motor efficiency η_{EM}.

$$\sum_{j=1}^{3} P_{Gj}\eta_G = \frac{P_{hotel}}{\eta_{trans}} + \sum_{j=1}^{2} \frac{P_{EMj}}{\eta_{EM}\eta_{VFD}} \tag{23}$$

The VFDs, as shown in Figure 5, also ensure that the power target setting P_{set} is reached while also being constrained by a certain power ramp rate. Based on the rotational speed of the motor N, the VFDs also enforce that the torque and power limits $P_{EM,lim}$ of the motors and converters are not exceeded, after which the electric motor torque M_{EM} is directly calculated based on the current shaft speed and (mechanical) motor power P_{EM}, as presented by equations 24 and 25.

$$P_{EM} = min(P_{set}, P_{EM,lim}(N)) \tag{24}$$

$$M_{EM} = \frac{P_{EM}}{N\frac{\pi}{30}} \tag{25}$$

3.6.2 Propeller and hull

To simulate ship performance, the mechanical power provided by the electric motors is converted into propeller thrust, providing the driving force for the hull of the ship. The model is considering both the rotation mechanics (i.e. the shaft lines), and the translation mechanics (i.e. hull and ship mass). The torque balance in the rotational domain is presented by equation 26, where inertia I dictates how quickly shaft speed ω can change, depending on the difference between propeller torque M_{prop} and electric motor torque M_{EM}.

$$I\frac{d\omega}{dt} = M_{EM} - M_{prop} \tag{26}$$

Similarly, the force balance in the (1-DOF) translation domain is presented by equation 27. Here, the ship's speed v_{ship} depends on its mass M, the propeller thrust T_{prop}, the number of propellers k_p, and the speed dependent ship resistance R_{ship}. A thrust deduction factor t is included to compensate for propeller-hull interactions.

$$M\frac{dv_{ship}}{dt} = k_p T_{prop}(1-t) - R_{ship}(v_{ship}) \tag{27}$$

Propeller thrust T_{prop} and torque M_{prop} are calculated using the four quadrant representation of propeller performance data, presented in equations 28 and 29, where thrust coefficient C_T and torque coefficient C_Q are obtained from the propeller performance diagrams. The density of the surrounding (sea)water ρ and propeller diameter D are constants. Wake fraction w relates the ship speed to the advance speed v_a, the velocity of the inflowing water as observed by the propeller, as presented by equation30. Shaft speed N is equal to shaft speed ω after accounting for unit conversion (i.e. from $[rpm]$ to $[rad/s]$).

$$T_{prop} = C_T(v_a{}^2 + (0.7\pi\frac{N}{60}D)^2)\rho\frac{\pi}{8}D^2 \tag{28}$$

$$M_{prop} = C_Q(v_a{}^2 + (0.7\pi\frac{N}{60}D)^2)\rho\frac{\pi}{8}D^3 \tag{29}$$

$$v_a = (1-w)v_{ship} \tag{30}$$

All parameters related to propeller and hull models, including ship resistance and hull interaction parameters, are directly based on the work of Geertsma (2019) without any further modifications. Propeller performance data is based on the well-known Wageningen (C5-75) C-series stock propeller Dang et al. (2013).

3.7 Controls

To realise the power transients for the nuclear power plant, controllers must be added. Not only should controllers change the power output of the system, but controls should also ensure operating conditions within the cycle do not impact the dynamic load changes of the cycle, and keep the cycle within safe limits. Therefore, controls are categorised in safety control, which includes main compressor inlet temperature control, compressor in- and outlet pressure control and reactor temperature control, and load controls includes bypass control, reactor control, and power control of the propulsion electric motors. If controllers are implemented in the model, a version of a PID controller has been selected, which has been tuned manually.

3.7.1 Safety control

Near the critical point of CO_2 do slight operating conditions result in drastic thermophysical property changes. As the operating region of the main compressors is the closest to the critical point, it is of importance to control the inlet conditions to ensure a stable working regime. To control the inlet temperature of the main compressor, a PID controller adjusts the mass flow through the cooler Bian et al. (2022).

Furthermore, throttle valves are placed around the compressor to ensure a stable and safe operating regime. Before the compressors, the valves ensure that the flow entering the compressors has a pressure of 90 bar, equal to the lower cycle pressure. Throttle valves placed after the compressors ensure that the cycle pressure does not exceed the maximum cycle pressure of 250 bar Olumayegun and Wang (2019). In addition, the throttle valve after the recompressor ensures the flow entering the mixer has the same pressure as after the LTR, preventing flow reversal that could damage the machinery Carstens (2007).

To control the reactor temperature, two control systems are present. At first, the addition of a dump cooler before the reactor controls the reactor inlet temperature, acting the same as the main compressor inlet temperature controller. Second, the control rods of the reactor can be used to control the reactor output temperature, limiting the power output of the reactor if the temperature increases.

3.7.2 Load control

Firstly, reactor control is performed by raising or lowering the control rods, based on the required power output of the reactor. As one controller cannot control two different things, using this option will reduce the option for reactor temperature outlet control. Furthermore, the speed of the control rods is tightly regulated to provide a stable power transient of the reactor Atkinson et al. (2021). If the controls rods were raised too fast, the reactor could turn prompt critical. As this results in an uncontrolled and rapid increase of fission reactions, and thus power increase, the consequence could be severe overheating that can lead to a meltdown or explosion, which should be prevented in all cases Duderstadt and Hamilton (1976).

Secondly, bypass control is used by implementing a bypass valve parallel to the turbine. This is a common bypass location for steam cycles. Although other bypass locations could be beneficial Carstens (2007)Wang et al. (2021)Wien (2024), for simplicity this common bypass location was selected. The bypass valve controls the shaft speed of the power conversion cycle. As a change in load power will result in a change in shaft speed according to equation 20, this results in that bypass control indirectly controls the power output of the cycle Bian et al. (2022). Opening the bypass will result in a reduction of mass flow entering the turbine, this way lowering the power output of the turbine. If the cycle operates at maximum power, the bypass should be fully closed to ensure maximum mass flow enters the turbine for maximum power production.

Lastly, the electric load demand is regulated using power electronics which are capable of following a fixed and prescribed power ramp. The overall electric load demand consists of two components, 1) the power required by the two electric propulsion motors, and 2) the power required by hotel and ship service loads. For the hotel and services loads, the required electrical power is assumed to be constant and is therefore not actively controlled. Variable frequency drives feeding the electric motors ensure that the propulsion load is controlled, reaching the desired power target while not exceeding the desired ramp rates.

4 Scenario description

4.1 Scenario introduction

To determine the dynamic behaviour of the nuclear power plant installation, it is of importance to investigate different scenarios. A distinction will be made between three different scenarios, of which an overview is presented in Table 4. Scenario 1 investigates the possibility of dynamic power control based on the transient of the reactor. Here, the reactor operates at low power and will increase its power based on the demanded power increase of the vessel. Scenario 2 investigates the possibility in which the reactor operates at constant power level and the dynamic power demand is realised by the secondary cycle. Bypass control will here solely control the load demand, but in this case the dump cooler placed in the primary circuit will not be present. Finally, scenario 3 will also operate with constant reactor power and a dynamic power change in the secondary cycle, but in this case a preliminary dump cooler will be added to the system ensuring reactor temperature control.

Table 4: Scenario conditions

Scenario	#1	#2	#3
Control			
Main compressor inlet temperature	Yes	Yes	Yes
Throttle valves (V1-V4)	Yes	Yes	Yes
Bypass valve (V6)	Yes	Yes	Yes
Reactor temperature inlet/outlet	No	No	Yes
Power transient			
Load speed	Fast as possible	Slow (0.75%/s)	Fast (3.00%/s)
Nuclear reactor output	Controlled	Fixed	Fixed
Dump cooler active (V5)	No	No	Yes

4.2 Ship manoeuvres

The three different scenarios will be investigated based on specific ship manoeuvres. It was decided to only look at a full linear power demand going low-high-low (10%-100%-10%), as this presents the most challenging power transient of a naval vessel. For the vessel, the 10% only corresponds to the load of hotel and ship services (base load) and the increase of 90% corresponds to accelerating from zero propulsion power to full propulsion power. To determine if a nuclear power plant installation can achieve similar power dynamics to conventional prime movers, two different transient speeds will be investigated. As the diesel engine and the gas turbine are the most common types of prime movers of a naval vessel, these will act as comparison for the transient speed of the system. It is common for a diesel engine to achieve 10-100% load changes in 120 seconds, while the transient of a gas turbine is even faster, being capable to achieve a load transient of 10-100% in 30 seconds. Therefore, this paper will apply two power transients to test the dynamic possibilities of the different scenarios; a slow transient of 0.75%/s and a fast transient of 3.00%/s. Note that these values are generic and aim to represent what is considered typical engine performance for naval applications, and do not include the impact of specific control strategies or any type-specific modifications made to the engines.

5 Results

5.1 Reactor limitations

Within this scenario, the power dynamics of the reactor will be presented in combination with a bypass. The reactor is limited in its dynamics, by the previous mentioned control rod speed, and therefore the bypass is implemented to control the shaft speed. The simulation applies the maximum allowed control rod speed if the power demand on the cycle changes. If this change in power of the reactor is not sufficient, then bypass control will aid the power dynamics as much as possible. It was decided to limit the speed of the load in such a way that the shaft speed does not change more than 3%, as this indicates the limits of the bypass within the created scenario.

As a result, the power transient presented in Figure 8 can be achieved. Here, the power transient corresponding to the diesel engine and gas turbine are plotted for reference. The power transient presented in Figure 8a starts at 300 seconds and ends at 650 seconds. Within this time frame, a power change of 90% is realised compared to the rated power, resulting in a power transient of 15.4%/min. This is however the result of bypass and reactor control operating at the same time. Solely looking at the reactor power output of the simulation, presented in Figure 8a, the simulated ramp rate of the reactor is approximately 4.6%/min. This corresponds to ramp rate values presented in literature of VHTRs, which are between 3-10% min IAEA (2022) IAEA (2023) NRG (2023). Although the implementation of the bypass increases the ramp rate of the reactor slightly, it is not able to come close to the required power dynamics of a naval vessel.

It must be noted, that during the simulation, the power dynamics of this scenario are limited by the first stage of the power transient, which goes from 10-100% cycle power. At the start of the scenario, the reactor is scaled down in power output as the cycle is operating in part load. Although this is beneficial for cycle efficiency, as less heat will be produced that will just be wasted, it also results that during the load increase the reactor must increase its thermal power output. Increasing reactor power output is strictly limited by the reactor dynamics and as a result faster power dynamics cannot be achieved by the bypass. To limit the impact of the reactor dynamics, the next scenario will discuss power transients during stable reactor power.
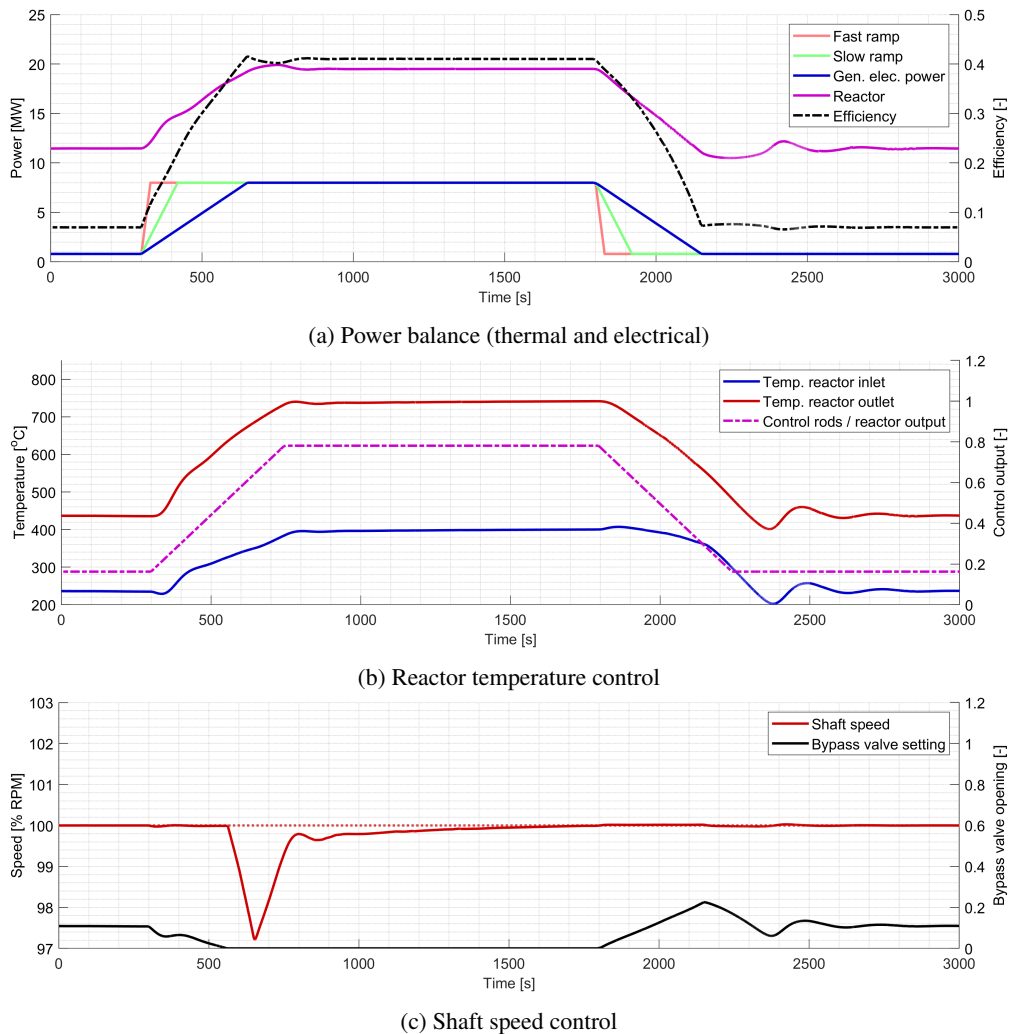
(a) Power balance (thermal and electrical)

(b) Reactor temperature control

(c) Shaft speed control

Figure 8: Simulation results scenario 1, reactor limitations

5.2 Secondary cycle performance

As scenario 1 indicates that the dynamics of the reactor are the limiting factor for the power transient, scenario 2 tries to achieve the power transient with a constant reactor control. To realise constant reactor control, the height of the control rods will be constant at the level belonging to a reactor output of 20 MWth. This limits the influence of the reactor dynamics on the system, but the secondary cycle is now responsible for achieving the required power dynamics, which is realised by the bypass valve controlling the mass flow through the turbine.

The results of the power transient are presented in Figure 9. Here, the slower ramp rate of the diesel engine is tested on the power conversion cycle, and the model is capable to run the simulation before large shaft speed changes start to occur. At full cycle power, the reactor produces its expected power of 20 MWth, as the secondary cycle is now absorbing all the required heat of the reactor. As a result, the inlet and outlet temperature of the reactor are within the expected region of 400°C and 750°C respectively. However, although the control rods are maintained at the same height, the power of the reactor does not stay constant if the cycle enters part load. This is the result as temperature control on the reactor is not guaranteed. During low part load, not all the heat produced in the reactor is used by the power conversion cycle. Although cooling power starts to increase slightly, most of the heat is returned to the reactor through the recuperators, resulting in an increased inlet and outlet temperature at the reactor side. This pushes the reactor into a temperature region for which it is not designed, as the temperature at the inlet of the reactor increases up to 590°C. As shown in Figure 2, the helium flows between the outer wall of the reactor barrel and the inside of the reactor pressure vessel before entering the reactor core, effectively cooling the reactor barrel and preheating the helium. Atkinson et al. (2019a) states that the temperature of the reactor barrel should not exceed 425°C, as material regulations imposed by the ASME state that graphitization of steel occurs at these temperatures. Therefore, the inlet temperature of helium is limited to around 400°C at steady state, but according to Figure 9b these safety limits are (excessively) breached during power transients.

Compared to scenario 1, is scenario 2 able to provide the power dynamics corresponding to the transient of a diesel engine, due to operating the reactor at constant level. However, the temperature limits of the reactors are exceeded as reactor temperatures are not controlled. Because of this, scenario 3 will continue by operating the reactor at constant power, but will add additional temperature control for the reactor.
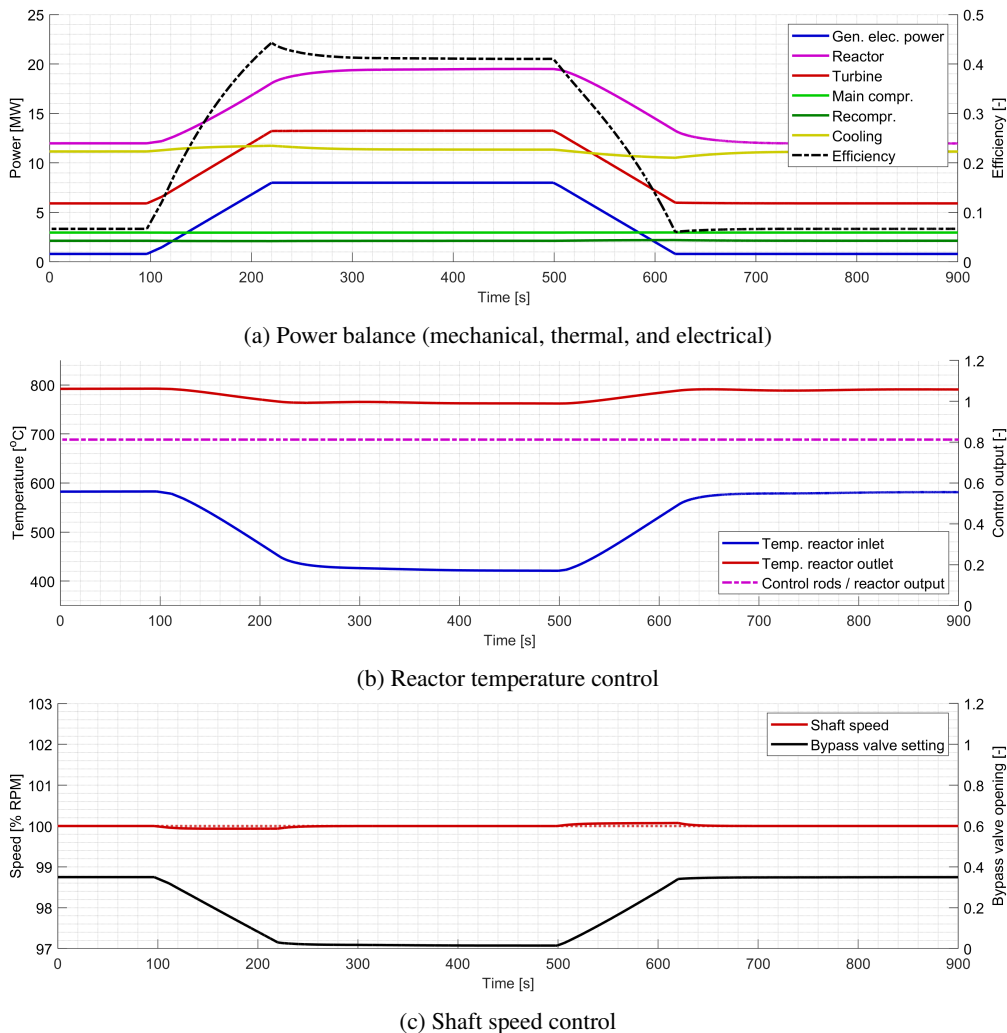

(a) Power balance (mechanical, thermal, and electrical)

(b) Reactor temperature control

(c) Shaft speed control

Figure 9: Simulation results scenario 2, bypass control with fixed reactor output

5.3 Dynamics of a nuclear vessel

5.3.1 Impact of the dump cooler

Scenario 2 shows that the power transient of the diesel engine cannot be achieved without exceeding safe temperature values within the reactor. Still, it seems possible to achieve the desired power transients and therefore a preliminary design solution has been implemented to limit the temperature increase within the reactor. A dump cooler has been added to the system to control the inlet temperature of the reactor. Furthermore, the control rods will be used to control the temperature outlet of the reactor, ensuring that the temperatures, and thus power output, of the reactor stays stable. To test the dynamic limits of this system, the simulation results belonging to a fast power transient ramp are presented in Figure 10.

This scenario gives promising results as not only the ramp rate of a diesel engine, but also the fast power transient of a gas turbine can be achieved with the nuclear power plant installation. The bypass control, in combination with the turbine, achieves the required power dynamics while the dump cooler prevents large temperature swings and ensures a stable reactor temperature at the inlet. Due to this relative stable inlet temperature at 400°C, the control rods of the reactor are capable to maintain the outlet temperature of the reactor stable around 750°C, resulting in no violation of the temperature limits. However, as can be seen in Figure 10a, the dump cooler must waste a lot of heat, resulting is low cycle efficiencies during part load, which is the result of constant reactor operation.

Within Figure 10a a small decrease in power dynamics can be observed near operating at full cycle power. This is however not a limitation of the nuclear power plant, but the result of dynamic limitations due to the performance of the vessel. To give insight into these limitations, scenario 3 has been performed an additional time, but now comparing ship performance between a slow and fast transient.
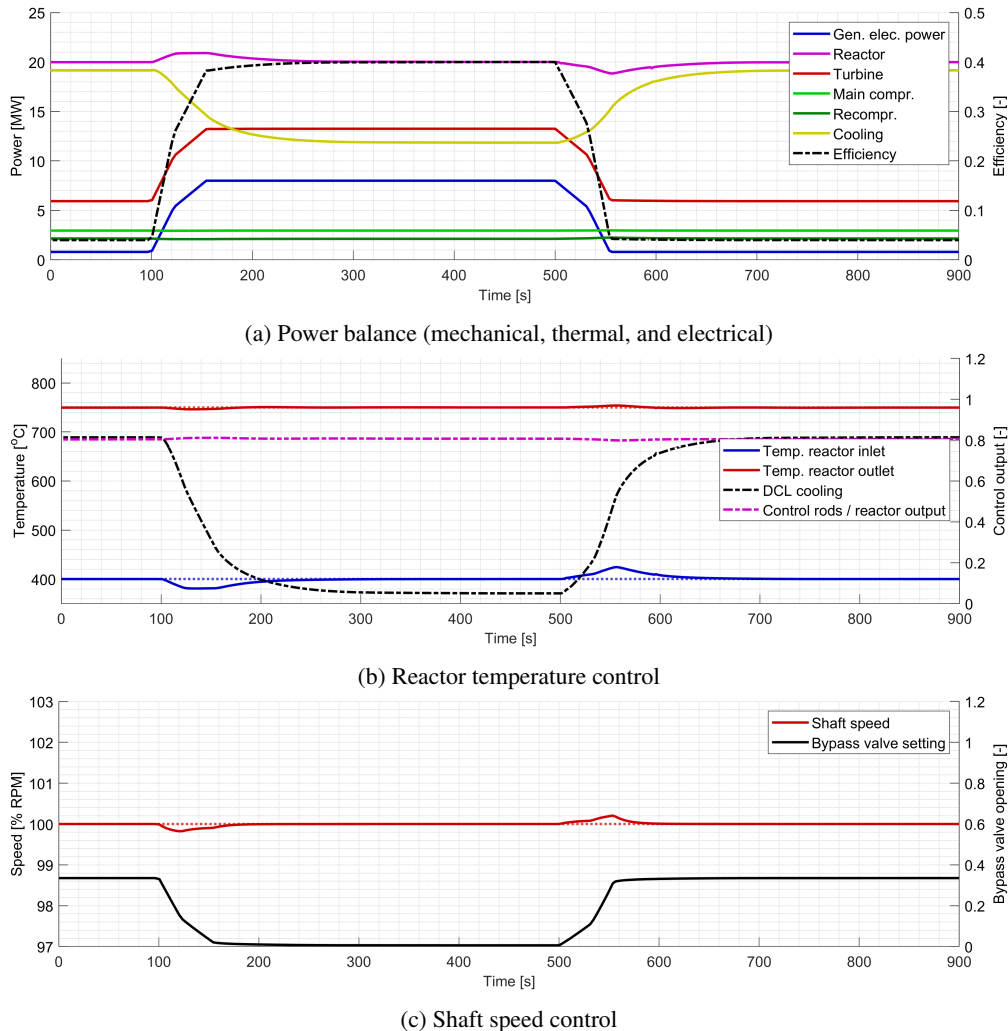

(a) Power balance (mechanical, thermal, and electrical)

(b) Reactor temperature control

(c) Shaft speed control

Figure 10: Simulation results scenario 3, bypass control with dump cooler

5.3.2 Impact of ship performance

To explain the small decrease in dynamics near full cycle power, the power rate of the diesel engine and the gas turbine will be implemented on the cycle as designed in scenario 3. The results of this comparison on ship performance level are presented in Figure 11. Here, the speed of the ship reaches 95% of its maximum speed in 85 and 125 seconds for the fast and slow power transient respectively. The acceleration also differs, as the acceleration reaches $0.24 \frac{m}{s^2}$ at 20 seconds during the fast transient, while the slow transient reaches a maximum acceleration of $0.14 \frac{m}{s^2}$ after 50 seconds.

Looking at Figure 11d, the performance of the electric motor is also presented. During the slower transient, the shaft speed increases gradually and therefore does not reach the limits of the motor before it reaches full mechanical power. The fast transient however, accelerates the shaft faster and therefore the transient limits of the electric motor are reached. This translates itself in Figure 11c to a motor torque that flattens for a certain time period, limiting the power dynamics of the whole vessel. After operating for around 30 seconds with at a flatten torque level, the motor passes its nominal point and enters constant power operation.
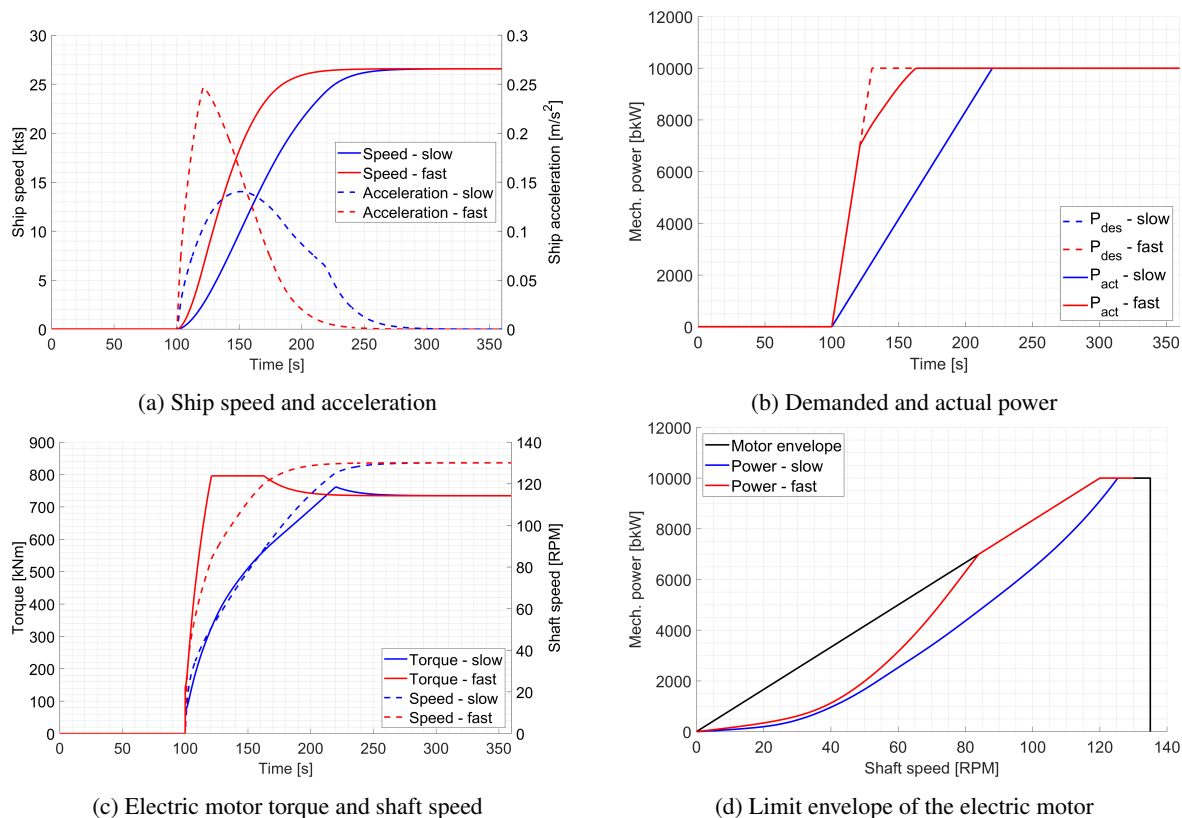
(a) Ship speed and acceleration

(b) Demanded and actual power

(c) Electric motor torque and shaft speed

(d) Limit envelope of the electric motor

Figure 11: Ship performance simulation results, comparing slow and fast power ramps

6 Conclusions and further research

This paper investigates a very high temperature reactor (VHTR) in combination with a supercritical carbon dioxide (sCO$_2$) power conversion cycle for implementation on a naval vessel. By presenting a novel dynamic power plant model of a nuclear reactor, its power conversion cycle and the ship propulsion systems, different ship manoeuvres could be investigated. Power transients of conventional prime movers, the diesel engine and gas turbine, were compared with the designed nuclear power plant to indicate the dynamic possibilities of nuclear power generation.

Using reactor control, even in combination with bypass control, to achieve the power transient of a naval vessel was deemed unsuccessful. If the reactor operates at part load, and the power demand increases, the system is limited by the dynamics of the reactor, and can not provide the required power transient. However, by using the reactor as a constant power load, and achieving the power dynamics with solely bypass control, realises that fast power transient up to gas turbine level can be achieved. This requires however implementation of additional systems on a design level, like the proposed dump cooler, to ensure reactor temperatures are maintained within a safe region. Furthermore, the dynamic performance of the nuclear power plant was not deemed the limiting factor during ship transients, but the limitation occurs in the operating envelope of the electric motor.

The proposed bypass power control results in significantly low cycle efficiencies during part load. If the captain of the vessel is certain a fast power increase is not necessary, then the power production of the reactors could be minimized, lowering the amount of waste heat and thus improving cycle efficiency. However, this is currently not deemed an acceptable choice if there is uncertainty about a possible power transient, as then the transient of the reactor will limit the power transient of the whole vessel. As a result, there is a trade-off between a (relative) high efficiency at part load and the possibility of high power dynamics from the system.

The results of this paper indicate that there are still improvement possibilities regarding the design of a naval nuclear power plant. The balance between efficiency and dynamics will be critical to achieve economically viable and publicly supported nuclear vessels, which can still operate in high combat environments that require fast power dynamics. A nuclear power plant, generally viewed as a more slow and constant power source, is however capable to achieve the power transients of current naval vessels, and is therefore still deemed a feasible and attractive solution for the decarbonization of the maritime sector.

7   Recommendations

This paper focuses on the dynamic possibilities of a nuclear reactor, specifically the VHTR, in combination with an indirect sCO_2 recompression cycle, for naval applications. The authors believe this reactor and power conversion cycle combination is a promising concept option for nuclear power generation, but other philosophies could change the type of reactor or power conversion cycle. This could impact the dynamic behaviour of the nuclear power plant. The main points of this paper should however be valid, as the authors do not see the possibility of improving the dynamics of the components in such a way that results would differ significantly. Still, further research should indicate the maximum dynamic performance of different systems within the cycle, which are especially unknown for a nuclear reactor designed with a focus on dynamic performance.

Furthermore, the models created are focused on implementing existing design technologies for accuracy. Although a preliminary design study, based on scaling assumptions, has been performed on the nuclear reactor, its power conversion cycle and the vessel, a full design study was not performed due to a lack of time. A thorough design study could give additional insights towards the dynamic behaviour of the power plant and is therefore recommended. This is however only beneficial if certain aspects like the type of vessel and the type of reactor are selected, as otherwise the differences between different cycle configurations is too significant.

The paper presents a dump cooler as a solution for the increase in reactor temperature during part load. This is however a preliminary design solution and results in an increase in the amount of heat wasted to the seawater. Further studies could therefore produce other design solutions or control strategies to increase the overall cycle performance, especially during part load, while maintaining the possibility of high power dynamics. The implementation of inventory control is a very promising option in this regard, as this presents a solution for dynamic power control with higher cycle efficiencies. A variable split ratio could also improve part load efficiency. In addition, thermal and electrical energy storage should be carefully investigated to ensure waste energy is minimized. Thermal energy storage could be realized by inserting a molten salt loop between the reactor and the secondary cycle, creating a buffer against large load transients in the secondary cycle and allowing the reactor more time to respond to load changes. Electrical energy storage will introduce the possibility of peak shaving, ensuring that large load transients caused by propulsion, DEW, pulse loads, or otherwise, are not directly transferred to the nuclear power generator units.

Finally, the authors tried to the best of their knowledge to indicate, and propose solutions, for safety issues during power transients of the system. They are however not specialised within material compositions or safety evaluations of nuclear systems, and a full safety evaluation of the different cycle components during the power transients should be performed by experts. This could indicate if other safety issues are present during the dynamic power transient and if changes to system design are required.

Declaration of competing interest

The authors declare that there is no conflict of interest that could have influenced the work reported in this paper. Furthermore, the authors of this paper would like to note that the views and beliefs presented within this paper are solely their views and beliefs, and do not necessarily reflect the views and beliefs of Damen Naval and/or the Royal Netherlands Navy.

Acknowledgements

Nomenclature

Symbols					
			Λ	Prompt neutron generation lifetime	$[s]$
β	Delayed neutron fraction	$[-]$	λ	Effective decay constant	$[s^{-1}]$
ΔH	Height difference	$[m]$	ω	Shaft speed	$[\frac{rad}{s}]$
$\dot{m}$	Mass flow	$[\frac{kg}{s}]$	π	Pressure ratio	$[-]$
η	Efficiency	$[-]$	ρ	Density	$[\frac{kg}{m^3}]$
γ	Specific heat ratio	$[-]$	ρ	Reactivity	$[\$/pcm]$

A	The heat transfer area	$[m^2]$
C	Specific heat capacity	$[\frac{J}{kgK}]$
c	Concentration of a delayed neutron group	$[-]$
C_v	Valve coefficient	$[-]$
C_Q	Propeller torque coefficient	$[-]$
C_T	Propeller thrust coefficient	$[-]$
D	Propeller diameter	$[m]$
d_H	Hydraulic diameter	$[m]$
f	Friction factor	$[-]$
f_{map}	Performance map function	$[-]$
f_{open}	Valve opening	$[-]$
g	Acceleration due to gravity	$[\frac{m}{s^2}]$
h	Enthalpy	$[\frac{kJ}{kg}]$
h	Heat transfer coefficient	$[\frac{W}{m^2K}]$
I	Inertia	$[kgm^2]$
k	Thermal conductivity	$[\frac{W}{mK}]$
k_p	Number of propellers	$[-]$
L	Length	$[m]$
M	Mass	$[kg]$
M	Torque	$[Nm]$
N	Shaft speed	$[RPM]$
n	Neutron population	$[-]$
P	Power	$[W]$
p	Pressure	$[Pa]$ or $[bar]$
Q	Heat	$[J]$
R	Resistance	$[N]$
s	Entropy	$[\frac{kJ}{kgK}]$
T	Temperature	$[^oC]$
T	Thrust	$[N]$
t	Thrust deduction factor	$[-]$
t	Time	$[s]$
t_e	Equivalent thickness	$[m]$
U	Overall heat transfer coefficient	$[\frac{W}{m^2K}]$
u	Speed	$[\frac{m}{s}]$
v	Ship speed	$[knots]$
v_a	Advance speed	$[m/s]$
w	Wake factor	$[-]$
Nu	Nusselt number	$[-]$

Abbreviations

B	Blower
CL	Cooler
DCL	Dump cooler
DEW	Direct energy weapons

DOF	Degrees of freedom
EM	Electric motor
FPP	Fixed pitch propeller
G	Generator
HEU	High enriched uranium
HTR	High temperature recuperator
IHX	Intermediate heat exchanger
LEU	Low enriched uranium
LTR	Low temperature recuperator
MC	Main compressor
P	Pump
P/D	Pitch over diameter ratio
PWR	Pressurised water reactor
R	Reactor
RC	Recompressor
RPV	Reactor pressure vessel
sCO_2	Supercritical carbon dioxide
T	Turbine
TAC	Turbine-Alternator-Compressor
TRISO	Tri-structural isotropic
TRL	Technology readiness level
TTD	Terminal temperature difference
U-235	Uranium 235
UO_2	Uraniumdioxide
V	Valve
VFD	Variable frequency drive
VHTR	Very high temperature reactor

Subscripts

c	cold side
corr	corrected
h	hot side
hotel	hotel and ship service (loads)
i	inlet
isen	isentropic
j	index counter
lim	limit(ed) value
n	node
o	outlet
prop	propeller
set	setpoint
ship	ship-related property
trans	transformer
w	wall

References

Alsawy, T., Mohammed, R.H., Mesalhy, O., Elsayed, M.L., 2024. Dynamic performance of supercritical co2 brayton cycle and its relationship to the correction of turbomachinery performance maps: A comparative analysis. Applied Thermal Engineering 242, 122364.

Atkinson, S., 2018. Design variances and optimisation of the U-Battery. Ph.D. thesis. University of Sheffield.

Atkinson, S., Abram, T.J., Litskevich, D., Merk, B., 2019a. Small modular high temperature reactor optimisation – part 1: A comparison between beryllium oxide and nuclear graphite in a small scale high temperature reactor. Progress in Nuclear Energy 111, 223–232.

Atkinson, S., Aoki, T., 2024. The development of a fuel lifecycle reactivity control strategy for a generic micro high temperature reactor. Nuclear Engineering and Technology 56, 785–792.

Atkinson, S., Aoki, T., Litskevich, D., Merk, B., Xing, Y., 2021. Part 3: Evaluating a small modular high temperature reactor design during control rod withdrawal and a depressurised loss of coolant accidents. Progress in Nuclear Energy 134, 103689.

Atkinson, S., Litskevich, D., Merk, B., 2019b. Small modular high temperature reactor optimisation part 2: Reactivity control for prismatic core high temperature small modular reactor, including fixed burnable poisons, spectrum hardening and control rods. Progress in Nuclear Energy 111, 233–242.

Bian, X., Wang, X., Wang, R., Cai, J., Tian, H., Shu, G., Lin, Z., Yu, X., Shi, L., 2022. A comprehensive evaluation of the effect of different control valves on the dynamic performance of a recompression supercritical co2 brayton cycle. Energy 248, 123630.

Brun, K., Friedman, P., Dennis, R., 2017. Fundamentals and Applications of Supercritical Carbon Dioxide (SCO2) Based Power Cycles. Woodhead Publishing.

Carstens, N.A., 2007. Control Strategies for Supercritical Carbon Dioxide Power Conversion Systems. Ph.D. thesis. Massachusetts Institute of Technology.

Dang, J., Van den Boom, H., Ligtelijn, J.T., 2013. The wageningen c-and d-series propellers, in: 12th International Conference on Fast Sea Transportation FAST, Citeseer.

Deng, T., Li, X., Wang, Q., Ma, T., 2019. Dynamic modelling and transient characteristics of supercritical co2 recompression brayton cycle. Energy 180, 292–302.

Ding, M., Kloosterman, J.L., Kooijman, T., Linssen, R., Abram, T., Marsden, B., Wickham, T., 2011. Design of a U-Battery. `https://www.janleenkloosterman.nl/reports/ubattery_final_201111.pdf`. Accessed on: 21-03-24.

Dostal, V., 2004. A Supercritical Carbon Dioxide Cycle for Next Generation Nuclear Reactors. Ph.D. thesis. Massachusetts Institute of Technology.

Duderstadt, J.J., Hamilton, L.J., 1976. Nuclear reactor analysis.

Dutch maritime sector, 2023. No guts, no Hollands Glorie! `https://www.rijksoverheid.nl/documenten/rapporten/2023/10/26/sectoragenda-mmi`. Accessed on: 21-03-24.

Freire, L.O., de Andrade, D.A., 2015. Historic survey on nuclear merchant ships. Nuclear Engineering and Design 293.

Furlong, A.J., Ge, H., Hughes, R.W., Macchi, A., Haelssig, J.B., 2024. Dynamic modelling of cross-flow printed circuit heat exchangers for multistage reactor intercooling. Applied Thermal Engineering 239, 122010.

Geertsma, R.D., 2019. Autonomous Control for Adaptive Ships with Hybrid Propulsion and Power Generation. Ph.D. thesis. Delft University of Technology.

Gen IV International forum, 2014. Technology roadmap update for generation iv nuclear energy systems. `https://www.gen-4.org/gif/upload/docs/application/pdf/2014-03/gif-tru2014.pdf`. Accessed on: 21-03-24.

Henryk Anglart, 2011. Nuclear Reactor Dynamics and Stability.

IAEA, 2022. Advances in Small Modular Reactor Technology Developments. `https://aris.iaea.org/sites/Publications.html`. Accessed on: 21-03-24.

IAEA, 2023. Advanced Reactors Information System(ARIS). `https://aris.iaea.org/sites/overview.html`. Accessed on: 21-03-24.

Jiang, Y., Liese, E., Zitney, S.E., Bhattacharyya, D., 2018. Design and dynamic modeling of printed circuit heat exchangers for supercritical carbon dioxide brayton power cycles. Applied Energy 231, 1019–1032.

Marchionni, M., Chai, L., Bianchi, G., Tassou, S.A., 2019. Numerical modelling and transient analysis of a printed circuit heat exchanger used as recuperator for supercritical co2 heat to power conversion systems. Applied Thermal Engineering 161, 114190.

Michael A. Pope, 2006. Thermal hydraulic design of a 2400 MWth direct supercritical CO2 cooled fast reactor. Ph.D. thesis. Massachusetts Institute of Technology.

Ming, Y., Liu, K., Zhao, F., Fang, H., Tan, S., Tian, R., 2022. Dynamic modeling and validation of the 5 MW small modular supercritical CO2 Brayton-Cycle reactor system. Energy Conversion and Management 253.

Ming, Y., Tian, R., Zhao, F., Luo, C., Tan, S., 2023. Control strategies and transient characteristics of a 5mwth small modular supercritical co2 brayton-cycle reactor system. Applied Thermal Engineering 235, 121302.

NRG, 2023. Small Modular Reactors 2023. `https://open.overheid.nl/documenten/ronl-7222d09bf81cec92c1c0b31f40133cf6fc7a6cea/pdf`. Accessed on: 21-03-24.

Oh, B.S., Lee, J.I., Kim, S.G., Cho, S.K., Yu, H., 2016. Transient analyses of s-co2 cooled kaist micro modular reactor with gamma+ code. The 11th International Topical Meeting on Nuclear Reactor Thermal Hydraulics, Operation and Safety Gyeongju .

Olander, D., 2009. Nuclear fuels – present and future. Journal of Nuclear Materials 389, 1–22.

Olumayegun, O., Wang, M., 2019. Dynamic modelling and control of supercritical co2 power cycle using waste heat from industrial processes. Fuel 249, 89–102.

Olumayegun, O., Wang, M., Kelsall, G., 2017. Thermodynamic analysis and preliminary design of closed brayton cycle using nitrogen as working fluid and coupled to small modular sodium-cooled fast reactor (sm-sfr). Applied Energy 191, 436–453.

Pham, H.S., Alpy, N., Ferrasse, J.H., Boutin, O., Tothill, M., Quenaut, J., Gastaldi, O., Cadiou, T., Saez, M., 2016. An approach for establishing the performance maps of the sc-co2 compressor: Development and qualification by means of cfd simulations. International Journal of Heat and Fluid Flow 61, 379–394.

Royal Dutch Navy, 2023. Sail Plan Vooruit! `https://open.overheid.nl/documenten/a45bdebd-7143-4a61-91f3-ebb357bf5d05/file`. Accessed on: 21-03-24.

Seatemperature.org, 2024. World Sea Temperatures. `https://www.seatemperature.org/`. Accessed on: 26-06-24.

Steigerwald, B., Weibezahn, J., Slowik, M., von Hirschhausen, C., 2023. Uncertainties in estimating production costs of future nuclear technologies: A model-based analysis of small modular reactors. Energy 281, 128204.

U.S. Department of Energy, 2024. Fuel Properties Comparison. `https://afdc.energy.gov/fuels/properties`. Accessed on: 21-03-24.

U.S. Department of the Navy and Department of Energy, 2015. The united states naval nuclear propulsion program. `https://shorturl.at/VWQU6`. Accessed on: 21-03-24.

Wang, X., Wang, R., Bian, X., Cai, J., Tian, H., Shu, G., Li, X., Qin, Z., 2021. Review of dynamic performance and control strategy of supercritical co2 brayton cycle. Energy and AI 5, 100078.

Wien, T.H., 2024. Nuclear Propulsion for Naval Vessels; investigating the dynamic behaviour of a nuclear powered super critical carbon dioxide power cycle. MSc. thesis. Delft University of Technology.

World nuclear association, 2023. World Nuclear Performance Report 2023. `https://www.world-nuclear.org/world-nuclear-performance-report.aspx`. Accessed on: 21-03-24.

Wu, P., Ma, Y., Gao, C., Liu, W., Shan, J., Huang, Y., Wang, J., Zhang, D., Ran, X., 2020. A review of research and development of supercritical carbon dioxide brayton cycle technology in nuclear engineering applications. Nuclear Engineering and Design 368, 110767.

van Zalk, J., Behrens, P., 2018. The spatial extent of renewable and non-renewable power generation: A review and meta-analysis of power densities and their application in the u.s. Energy Policy 123, 83–91.

Zohuri, B., 2020. Generation iv nuclear reactors. Nuclear Reactor Technology Development and Utilization , 213–246.